Tree Physiology 41, 2438–2453
https://doi.org/10.1093/treephys/tpab081

Methods paper

A double-ratio method to measure fast, slow and reverse sap flows

Zijuan Deng[1,4,5,†], Heather K. Vice[2], Matthew E. Gilbert[2], Mark A. Adams[3] and Thomas N. Buckley[2,†]

[1]Centre for Carbon, Water and Food, The University of Sydney, Brownlow Hill, NSW, 2570; [2]Department of Plant Sciences, University of California, Davis, CA 95616 USA; [3]School of Science, Faculty of Science, Engineering & Technology, Swinburne University of Technology, Victoria 3122, Australia; [4]Present address: College of Science and Engineering, Flinders University, Adelaide, Australia; [5]Corresponding author (zijuan.deng@flinders.edu.au, rosedeng0810@gmail.com)

Received October 8, 2020; accepted May 31, 2021; handling Editor Kathy Steppe

Sap velocity measurements are useful in fields ranging from plant water relations to hydrology at a variety of scales. Techniques based on pulses of heat are among the most common methods to measure sap velocity, but most lack ability to measure velocities across a wide range, including very high, very low and negative velocities (reverse flow). We propose a new method, the double-ratio method (DRM), which is robust across an unprecedented range of sap velocities and provides real-time estimates of the thermal diffusivity of wood. The DRM employs one temperature sensor upstream (proximal) and two sensors downstream (distal) to the source of heat. This facilitates several theoretical, heat-based approaches to quantifying sap velocity. We tested the DRM using whole-tree lysimetry in *Eucalyptus cypellocarpa* L.A.S. Johnson and found strong agreement across a wide range of velocities.

Keywords: double-ratio method, *Eucalyptus cypellocarpa*, heat-pulse-based technique, sap flow, sap flux, sap velocity, thermal diffusivity.

Introduction

Sap velocity measurements using heat-tracing techniques have been important means for studying plant water relations from whole plant to catchment scale in the tree physiology, forestry and hydrology communities (Wilson et al. 2001, Cermak et al. 2007, Buckley et al. 2011, 2012, Steppe et al. 2015). There are many heat-dissipation-based methods, but all have one or more weaknesses. Constant-power approaches such as the heat field deformation method (Nadezhdina et al. 1998) or Granier-style probes (Granier 1985) are inexpensive and robust but require empirical calibration (Clearwater et al. 1999) and consume large amounts of electrical power. Moreover, Granier-style probes cannot accurately measure small or negative sap velocities. A recent heat-pulse-based method, employing a single probe with finite heating duration (I-SPHP) (Lopez-Bernal et al. 2017), has advantages of low cost, simple fabrication and no requirement for correction of misalignment. However, that method cannot capture slow or negative flows, while an improved version, F-SPHP (Ren et al. 2020), broadens the measuring range to slightly negative flows but is more computationally intensive and sensitive to heat contamination. Both SPHP methods rely on a known thermal diffusivity (or conductivity) that requires independent measurements or calibration. Other heat-pulse-based methods such as the Tmax method (Cohen et al. 1981), compensation heat pulse method (CHPM) (Green and Clothier 1988), heat ratio method (HRM) (Burgess et al. 2001) and Sapflow+ method (Vandegehuchte and Steppe 2012*c*) use little power and are traceable to first principles, but also have limitations. Tmax and CHPM cannot measure low or negative velocities (Green et al. 2003, Vandegehuchte and Steppe 2012*c*), Sapflow+ suffers from difficulty in model identification, and the HRM fails at high sap velocities (Bleby et

†These authors contributed equally to this work.

al. 2008, Pearsall et al. 2014, Flo et al. 2019, Forster 2019, 2020).

In most heat-pulse-based methods, sapwood thermal diffusivity, k, is a crucial parameter in calculation of sap velocity (Vandegehuchte and Steppe 2012*a*, López-Bernal et al. 2014). An arbitrary value of k is usually set or obtained from empirical functions related to sapwood moisture content (m_c) (Marshall 1958, Burgess et al. 2001, Vandegehuchte and Steppe 2012*a*). However, k can change over seasons (Burgess et al. 2001, Chen et al. 2012) and even diurnally (López-Bernal et al. 2014), with uncertain consequences for the accuracy of calculated sap velocity. Velocity estimates from the Tmax method depend only on k and known parameters. Therefore, if sap velocity is known to be zero, k can be directly inferred and then treated as a constant until such a time that it can be re-calibrated (Burgess et al. 2001). Inverse modeling has also been used to calibrate k (Chen et al. 2012, Vandegehuchte and Steppe 2012*a*), notwithstanding measurement uncertainties and issues with probe alignment. For example, empirical functions to infer k from sapwood properties and m_c could be validated at low sap velocities under 20 cm h^{-1} (Vandegehuchte and Steppe 2012*b*); however, such procedures require knowledge of m_c, which may vary diurnally (López-Bernal et al. 2014). k has never been estimated *in vivo*, in real time, at higher sap velocities.

Pearsall et al. (2014) proposed a method for extending the range of sap velocities that can be reliably measured using heat-pulse approaches. They combined the HRM and CHPM, using the HRM to detect small and negative sap velocities and the CHPM to detect high sap velocities. A limitation of that approach is the lack of a non-arbitrary method for selecting whether to use the HRM- or CHPM-derived estimate of sap velocity at a given time. Another concern is alternation between very different measurement approaches: an average over time of velocity based on the ratio of temperature rises in two sensors (HRM), or inference based on estimation of the instant at which two temperature rises are equal (CHPM). Research communities that use sap velocity measurements thus lack a single method that is at once energy efficient, objective, robust and capable of measuring negative, low and high velocities with a single measurement principle.

We developed a new and efficient algorithm, the double-ratio method (DRM), that combines the strengths of existing methods and is robust across an unprecedented range of sap velocities, from moderate negative velocities to very large positive velocities. The DRM is an extension of the HRM in which an additional temperature sensor (Probe #3) is installed distal to (i.e., 'downstream' from, in the direction of normal diurnal flow) both temperature sensors used in the HRM. The DRM estimates sap velocity based on the same principles as the HRM—namely, by calculating the ratios of heat-pulse-induced temperature rises measured in different probes. Two different velocity estimates are produced—one based on Probes #2 and #1 (the upstream sensor and the first downstream sensor) and another based on Probes #3 and #2 (the two downstream sensors)—and the value with the lesser intrinsic uncertainty (which is calculated based on temperature rises and probe positions) is retained. Furthermore, the presence of a third sensor also enables CHPM estimates of flow, which can be combined with DRM-based estimates to allow real time estimation of k under high-velocity conditions. We tested the DRM experimentally using weighing lysimeters and examined its capability by numerical modeling. We discuss the strengths and weaknesses of the DRM in relation to other commonly used heat-pulse-based techniques.

Materials and methods

Theory

Background: heat pulse theory and the HRM Marshall (1958) showed that an instantaneous heat pulse at time $t = 0$ causes an increase in temperature (δ_i) at both axial (x_i) and azimuthal (y_i) positions relative to the heater at time t (s), with negative and positive x_i values indicating positions upstream relative to the heater (generally closer, more proximal, to stem base) and downstream relative to the heater (more distal to stem base):

$$\delta_i = \frac{Q}{4\pi\rho ckt}\exp\left(-\frac{(x_i - Vt)^2 + y_i^2}{4kt}\right), \quad (1)$$

where V is the heat pulse velocity in the axial direction (cm h^{-1}), Q is the total heat released per unit length of the heater (J m^{-1}), ρ is the sapwood bulk density (including water and wood) (kg m^{-3}), c is the sapwood heat capacity (J kg^{-1} K^{-1}) and k is the thermal diffusivity of the sapwood-water matrix (m^2 s^{-1}). Applying Eq. (1) to two probe locations, i and j, and rearranging provides an estimate of V:

$$V_{ij} = \frac{2k}{x_j - x_i}\ln\left(\frac{\delta_j}{\delta_i}\right) + \frac{x_i + x_j}{2t} - \frac{y_i^2 - y_j^2}{2t\,(x_j - x_i)}. \quad (2)$$

In Eq. (2), V is estimated from four types of quantities: a ratio of temperature increases between two probes (δ_j/δ_i), the thermal diffusivity k, the positions of the two probes (x_i, x_j, y_i, y_j), and the time elapsed since the heat pulse length (t). If the two probes are parallel to one another (i.e., at identical azimuthal positions relative to the flow axis), then $y_i = y_j$, giving

$$V_{ij} = \frac{2k}{x_j - x_i}\ln\left(\frac{\delta_j}{\delta_i}\right) + \frac{x_i + x_j}{2t}. \quad (3)$$

In the HRM, Eq. (3) is applied to two probes equidistant from the heater, one upstream (Probe #1, $i = 1$) and one downstream

(#2, $j = 2$), so that $x_1 = -x_2$ (where $x_2 > 0$), giving

$$V_{HRM} = V_{12} = \frac{2k}{x_2 - x_1} \ln\left(\frac{\delta_2}{\delta_1}\right). \quad (4)$$

A key strength of the HRM is that it can distinguish both small and negative heat pulse velocities (when sap flows in reverse, i.e., in an upstream or proximal direction, sap transfers heat towards Probe #1, causing $\delta_1 > \delta_2$ and hence $V_{12} < 0$).

Problems with high sap velocities in the HRM In practice, Eq. (4) is applied using experimental estimates of δ_1 and δ_2 ($\hat{\delta}_1 = \delta_1 + \varepsilon_1$ and $\hat{\delta}_2 = \delta_2 + \varepsilon_2$, respectively, where ε_1 and ε_2 are errors due to measurement noise, which can be either positive or negative, since they are presumably random and symmetrically distributed around zero). Applying these estimates to Eq. (4) gives

$$\hat{V}_{12} = \frac{2k}{x_2 - x_1} \ln\left(\frac{\hat{\delta}_2}{\hat{\delta}_1}\right) = \frac{2k}{x_2 - x_1} \ln\left(\frac{\delta_2 + \varepsilon_2}{\delta_1 + \varepsilon_1}\right). \quad (5)$$

When V_{12} is large, δ_1 is small (cf. Eq. (1)), and as a result the error term ε_1 becomes large relative to δ_1. If δ_1 is small enough, $\delta_1 + \varepsilon_1$ will be negative for some measurements (i.e., ε_1 will be negative and larger in magnitude than δ_1). Moreover, the proportion of such measurements will increase as δ_1 decreases, and hence as heat pulse velocity increases. Any algorithm to apply Eq. (4) must disregard such measurements, because they make the operand of the logarithm negative and thus undefined. But because ε_1 is negative for the discarded points, the remaining (undiscarded) estimates of δ_1 are positively biased, and hence the resulting estimates of V_{12} are negatively biased. This bias increases as the true velocity increases, which manifests experimentally as a 'plateau' or 'ceiling' in inferred heat pulse velocity (e.g., Figure 1), often in the vicinity of 30–50 cm h^{-1} (Pfautsch et al. 2011, Pearsall et al. 2014, Flo et al. 2019). The inferred velocity can actually decline even as true velocity continues to increase (Figure 1). Even if δ_1 is non-negative, noise in δ_1 at high velocities leads to the denominator of the heat ratio approaching zero, with the consequence that resulting estimates of V_{12} can fluctuate by orders of magnitude.

Principles of the DRM To alleviate the negative bias of the HRM at high V, we propose a new method, the DRM, that uses a three-step approach to estimate V. First, V_{12} is estimated as in the HRM. Second, an additional estimate of sap velocity (V_{23}, Eq. (6)) is computed using the temperature rises at Probes #2 and #3, where Probe #3 is located downstream to Probe #2 at the same distance as Probe #2 is from Probe #1 (so $x_3 = 3 \cdot x_2$):

$$V_{23} = \frac{2k}{x_3 - x_2} \ln\left(\frac{\delta_3}{\delta_2}\right) + \frac{x_2 + x_3}{2t}. \quad (6)$$

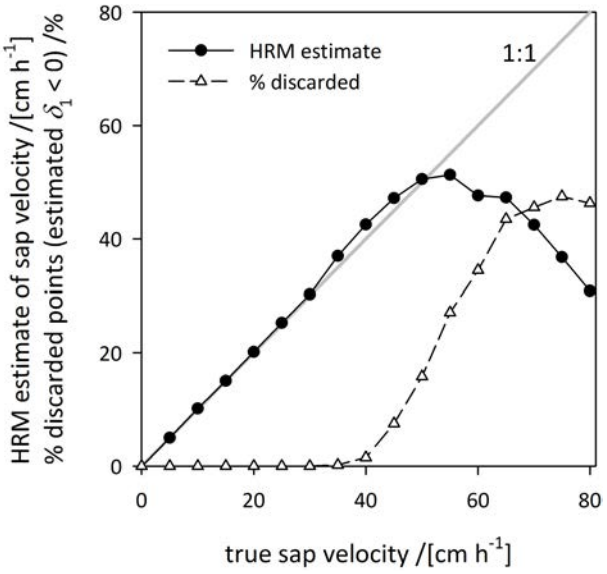

Figure 1. Example of negative bias in the HRM due to rejection, at high sap velocities, of points with negative estimates of temperature rise at upstream probe (δ_1). Closed symbols and solid black line: HRM estimate of sap velocity, open symbols and dashed line: % of points discarded due to negative δ_1 estimate. Monte Carlo simulation of Eq. (1) for $V = 0, 5, \ldots, 80$ cm h^{-1}, with $k = 0.0025$ cm^2 s^{-1} and $x_2 = -x_1 = 0.5$ cm and with ε_1 and ε_2 sampled from a normal distribution with mean 0 and $\sigma_T = 0.1$ K using Box-Muller transformation of 1000 uniform random deviates in [0,1] at each V.

The third step is to choose between the two estimates of velocity (V_{12} and V_{23}) to give a single, final estimate of V (V_{DRM}). On the grounds that measurements with less uncertainty are intrinsically preferable to those with greater uncertainty, we chose V_{DRM} as the value with the smaller intrinsic measurement uncertainty (σ_{12} or σ_{23}):

$$V_{DRM} = \begin{cases} V_{12} & \text{if } \sigma_{12} \le \sigma_{23} \\ V_{23} & \text{else} \end{cases}, \quad (7)$$

where σ_{12} and σ_{23} depend on the standard deviation of random noise for temperature sensors (σ_T) and on the estimated temperature rises at each probe (δ_1, δ_2 and δ_3), as follows:

$$\sigma_{12} = \frac{2k\sigma_T}{x_2 - x_1} \sqrt{\frac{1}{\delta_2^2} + \frac{1}{\delta_1^2}}, \text{and} \quad (8)$$

$$\sigma_{23} = \frac{2k\sigma_T}{x_3 - x_2} \sqrt{\frac{1}{\delta_3^2} + \frac{1}{\delta_2^2}}. \quad (9)$$

When the true velocity is negative or very low, the uncertainty in V_{23} will be greater than that for V_{12}, and V_{DRM} will equal V_{12}; conversely, at high velocities, $\sigma_{12} > \sigma_{23}$ and V_{DRM} will equal V_{23}. This selection procedure avoids the need to specify an arbitrary value of velocity at which to switch from one estimate to the other, as is required in the approach of Pearsall et al. (2014).

Note that, if the probes are evenly spaced (i.e., $x_3—x_2 = x_2—x_1$), then $\sigma_{12} > \sigma_{23}$ if $\delta_3 > \delta_1$, and vice versa; that is, V_{12} is chosen if $\delta_3 > \delta_1$, and V_{23} is chosen otherwise. An alternative approach, which we suggest for the sake of completeness but did not test here, would be to use the inverses of σ_{12} and σ_{23} as 'weights' to compute V_{DRM} as a weighted average of V_{12} and V_{23}, thus: $V_{DRM} = (V_{12}/\sigma_{12} + V_{23}/\sigma_{23})/(1/\sigma_{12} + 1/\sigma_{23})$.

Identifying the optimal time window for averaging velocity estimates In the HRM, V_{12} is computed as the average of repeated instantaneous estimates during a fixed period after the heat pulse. Burgess et al. (2001) suggest a 40-s time window, beginning 60 s after the pulse and ending at 100 s. The uncertainty-based approach of the DRM provides an alternative and objective way to identify the optimal time window: namely, by choosing the period that minimizes intrinsic uncertainty in velocity, computed as the standard error (SE) of the mean estimated velocity (based on the theoretical uncertainty in V_{DRM}, not the standard deviation of a sample of instantaneous estimates):

$$SE_{DRM} = \frac{1}{n_t}\sqrt{\sum_{t=a}^{b}\sigma_{DRM}^2(t)}, \quad (10)$$

where n_t is the number of time steps in the averaging window, σ_{DRM} is the lesser of σ_{12} and σ_{23} at each point in time, and the summation limits at right (a and b) denote the first and last steps in the averaging window. An efficient algorithm to minimize SE_{DRM} is to locate the moment of minimum σ_{DRM}, compute the SE_{DRM} for time windows of varying width around the moment, and choose the width that gives the smallest SE_{DRM}. We tested a variety of values for n_t.

Note that all equations were derived from Marshall's (1958) model (Eq. (1)) under the assumption of an instantaneous heat pulse, whereas in reality the heat pulse has a finite length of t_0. We corrected for this by shifting each temperature time-course by $-t_0/2$ before applying Eq. (1). The effect of this treatment is shown in Supporting Information Notes S1 and Figure S1 available as Supplementary data at *Tree Physiology* Online.

Theoretical test of the DRM, HRM, CHPM and Tmax methods

Comparison of heat-pulse-based methods To assess the theoretical viability of the DRM in comparison with other heat pulse methods (with similar probe settings), and to help optimize operational considerations such as the size and timing of averaging window(s), we used Eq. (1) to simulate time courses of temperature following a heat pulse. We compared the predicted values of V_{DRM} (Eq. (7)) with V_{HRM} (Eq. (4)), and also with two other estimates of V, based, respectively, on the CHPM (Green and Clothier 1988) and the Tmax method (Cohen et al. 1981), the latter as modified by Kluitenberg and Ham (2004). Using the CHPM, heat pulse velocities are calculated at the time point ($t_{C(1,3)}$) when temperature rises for Probes #1 and #3 are equal, so that the ratio of temperature rises is unity and the logarithmic term including k equals zero, giving the velocity as

$$V_{CHPM} = \frac{x_1 + x_3}{2t_{C(1,3)}}. \quad (11)$$

In the Tmax method, sap velocity is calculated from the time at which the measured temperature rise is greatest after a given heat pulse (t_m). This leads to

$$V_{Tmax} = \sqrt{\frac{4k}{t_0}\ln\left(1 - \frac{t_0}{t_m}\right) + \frac{x_i^2}{t_m\,(t_m - t_0)}}, \quad (12)$$

where x_i is the distance of the probe i from the heater (Probe #2 is typically used because it usually has the greatest peak temperature). Note that if the true sap velocity is known to be zero, Eq. (12) can be set equal to zero and rearranged to provide an estimate of k:

$$k = \frac{x_i^2}{4t_m}\left(\frac{t_0}{t_m - t_0}\right)\left(\ln\frac{t_m}{t_m - t_0}\right)^{-1}. \quad (13)$$

Simulations We performed two sets of simulations. In the first set, we simulated time courses of temperature rises for all three probes following a heat pulse, for sap velocities ranging from −10 to +80 cm h^{-1}. We added Gaussian noise with a standard deviation of 0.02 K (using simulation module *randn* in Matlab) to each time course. The procedures for generating the synthetic data in each time course, as well as estimated sap velocity, are provided in Methods S1 available as Supplementary data at *Tree Physiology* Online. Each such simulation was repeated 10^3 times to estimate the probability distribution of each estimate of sap flux under random temperature noise. All simulations used sapwood properties given in Table S1 available as Supplementary data at *Tree Physiology* Online, and heat pulse parameters and probe settings given in Table S2 available as Supplementary data at *Tree Physiology* Online.

In the second set of simulations (Methods S2 available as Supplementary data at *Tree Physiology* Online), we determined the sensitivity of each method to inaccuracy in k. While heat pulse methods typically assume constant k, in practice k varies with m_c, which may vary diurnally or seasonally in relation to changes in water potential and cycles of discharge and recharge of xylem water stores (Chen et al. 2012, López-Bernal et al. 2014). We simulated time courses of temperature rises as for the first set of simulations for sap velocities between −10 to +80 cm h^{-1}, while assuming each of three m_c values (0.5, 1.0, 1.5 g g^{-1}). We calculated k from m_c for a basic density (ρ_b) of $0.5{\cdot}10^3$ kg m^{-3} using the relationship given by Vandegehuchte and Steppe (2012*b*) (see

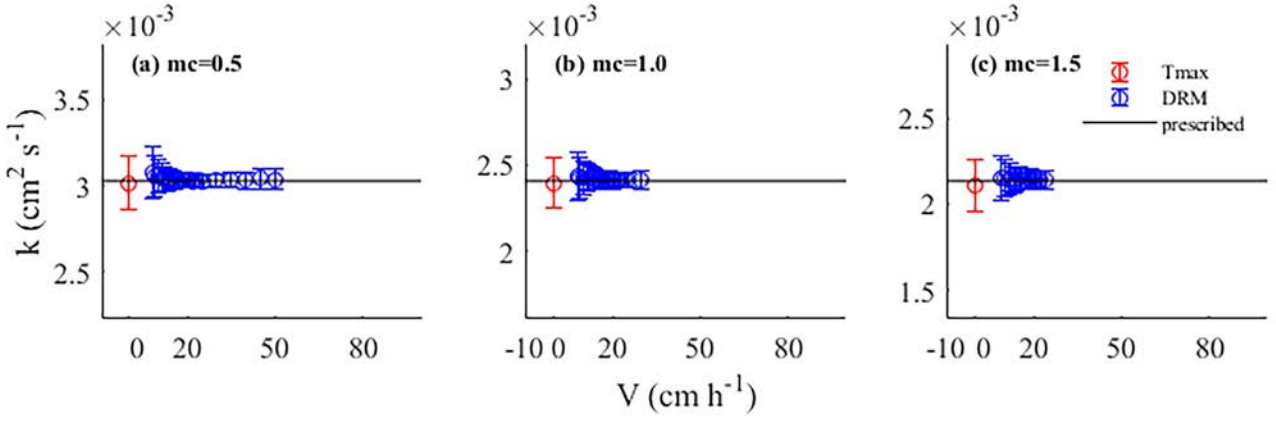

Figure 2. *k* estimation with the DRM (blue) and the Tmax (red). Error bars show the standard deviations of the calculated *k* with 1000 Monte Carlo samplings of Gaussian error; the black line shows the prescribed *k* at various moisture contents: (a) $m_c = 0.5$ g g^{-1}; (b) 1.0 g g^{-1}; (c) 1.5 g g^{-1}; *k* was estimated from m_c following Vandegehuchte and Steppe (2012*b*).

Figure S2 available as Supplementary data at *Tree Physiology* Online).

Theoretical test of internal calibration of k Because *k* may vary in relation to fluctuations in m_c, using a constant value of *k* in the DRM (or HRM) may cause systematic errors. To reduce such errors, *k* can be estimated *in vivo* by combining the sap velocity estimate from the DRM with an independent estimate of *V*, obtained from the CHPM, which does not explicitly depend on *k*. Although the CHPM itself has limitations (see Introduction), this procedure provides useful information about the magnitude of diurnal and seasonal changes in *k*. Setting V_{DRM} equal to V_{CHPM} under conditions of high sap velocity (so that $V_{DRM} = V_{23}$) and solving for *k* gives

$$k = \frac{(x_3 - x_2)(x_1 - x_2)}{4t_{C(1,3)} \ln\left(\frac{\delta_3}{\delta_2}\right)}, \qquad (14)$$

where the temperature rises δ_2 and δ_3 are those measured at time $t_{C(1,3)}$. The smallest sap velocity at which Eq. (14) applies depends on the probe spacing and recording time, which limit the range of sap velocities that can be measured using the CHPM (Eq. (11)). For example, for our recording time (400 s after the heat pulse) and probe spacing (1.5 cm between Probes #1 and #3), the lowest sap velocity that could be inferred from Eq. (11) would correspond with the temperature rises of Probes #1 and #3 crossing over at 400 s after the heat pulse, giving $V = (x_1 + x_3)/2t = (-0.75 + 2.25)/(2{\cdot}400) = 1.88{\cdot}10^{-3}$ cm s^{-1}, or 6.75 cm h^{-1}. The maximum *V* at which Eq. (14) applies depends on σ_T, *Q* and m_c. Figure 2 illustrates how the maximum discernible sap velocity varies with m_c for various probe and heat parameters (Table S2 available as Supplementary data at *Tree Physiology* Online). The drier the sapwood, the broader the range of velocities to which Eq. (14) applies because smaller m_c leads to larger *k*.

We estimated *k* as follows. First, we used Eq. (13) to estimate *k* prior to dawn, when sap velocity was negligible (as verified by lysimetry). We applied that value of *k* until *V* rose high enough (e.g., > 6.75 cm h^{-1}) in the early mornings for us to calculate *k* from Eq. (14). When *V* exceeded the range in which Eq. (14) is applicable (e.g., 50 cm h^{-1} in Figure 2a), we used the last estimated value of *k* until *V* fell again into a range in which Eq. (14) could be applied.

Validation of the DRM on trees

Lysimeter experiments We used whole-tree lysimetry to test the DRM, as well as the HRM, CHPM and Tmax methods. Measurements were made at the Centre for Carbon, Water and Food at the Camden Campus of the University of Sydney in Brownlow Hill, NSW, Australia (34.03°S, 150.66°E) in 2016–17. Three *Eucalyptus cypellocarpa* saplings, each in a large container (0.9 m by 1.2 m by 0.9 m), were placed on lysimeters capable of weighing up to 1200 kg (50 g resolution, Mettler Toledo, Columbus, Ohio). The three saplings were originally planted as seedlings in the containers in 2011. Irrigation was adjusted so that we could measure sap velocity across a range of water availabilities. Trees were initially irrigated for 30 min (around 2.5 l min^{-1}) twice a day for a month, and then reduced to 20 min twice a day, then to 2 min six times a day, and finally without any irrigation for several days. Transpiration was calculated from weight loss measured by the weighing lysimeters. Additional details regarding the lysimetry data analysis are provided in Methods S3. available as Supplementary data at *Tree Physiology* Online.

Sap velocity probe construction and installation Each probe set comprises three temperature sensor probes and one heater

probe. Each temperature sensor contained one thermistor (QTI Sensing Solutions, Boise, Idaho, E320) inserted into an 18-gauge blunt tip needle. Thermistor sensing tips were coated in heat sink compound before inserting and then centered 1.5 cm from the distal end of the needle. Thermistor depths were fixed by placing a drop of low-viscosity cyanoacrylate glue in both the proximal and distal end of the needle. Each heater was made by feeding approximately 65 cm of Manganin wire (Goodfellow Group Ltd, Coraopolis, Pennsylvania, CU065822) through a 27.5-gauge hypodermic needle, leaving 3 to 5 cm of wire extending from the proximal end of the needle with the remainder (approximately 60 cm) protruding from the distal end, and then winding the wire tightly around the outside of the needle until the distal 3 cm of needle was covered with winding. Cyanoacrylate glue was then applied to the proximal section of winding to prevent unwinding, and the needle's plastic base was removed by gripping the needle with pliers below the glued winding and bending it repeatedly at an angle of approximately 20° until it fractured and could be pulled off the remaining wire. The resulting 'heater core' was then dipped in heat sink compound and inserted into an 18-gauge needle. The total resistance of the heaters varied from 17 to 18.4 Ω and was insensitive to temperature between 0 and 70 °C. The sensors and heaters were soldered to extension cables, which were wired to an AM16-32B multiplexer (Campbell Scientific Inc., Logan, UT, USA) and relays, respectively. Initiation of the heat pulses and the temperature recordings were controlled by a CR850 datalogger (Campbell Scientific).

Probes were inserted radially into the sapwood and parallel to one another, with the aid of a portable drill press (Kanzawa, Miki, Japan, K-801) and a rigid guide plate made from angle iron and strapped to each tree. Temperature sensors were located at distances of 0.75 cm upstream (Probe #1, $x_1 = -0.75$ cm), 0.75 cm downstream (Probe #2, $x_2 = +0.75$ cm) and 2.25 cm downstream (Probe #3, $x_3 = +2.25$ cm) from the heater probe. One set of sensors was installed on each tree approximately 30 cm above the soil surface; the diameters of the trees (#1, 2 and 3) were 8.2, 8.4 and 10.0 cm, respectively, at the height of each heater probe. A heat pulse of 7–16 s in duration was initiated every 15 or 30 min by applying 12 V across the heater probe wire, which induced a peak temperature rise of around 2 K in Probe #2. The subsequent temperature change of each probe was recorded every second for 5 to 10 min. All probe installations were wrapped with 15-cm thick polyester insulation and covered with Mylar-coated bubble wrap for insulation.

The temperature rise (δ_i) was calculated by first computing the initial temperature of each probe as its average for 5 s before a given heat pulse. To account for drift in background temperature during the rise and decay of temperature following each heat pulse, we used the pchip function in Matlab to simulate changes in background temperature by smooth interpolation between each successive pre-heat-pulse initial temperature, and then subtracted the resulting changes in background temperature from each time course of temperature to give δ_i.

To validate the DRM with the mass flow rate (transpiration) measured by lysimeters, heat-pulse velocities (V, cm h^{-1}) were corrected for misalignment errors (see Methods S4 available as Supplementary data at *Tree Physiology* Online) and then converted to whole-tree sap flow (kg h^{-1}) following Burgess et al. (2001). Heat pulse velocity was first converted to sap flux density, V_s ('sap velocity on total sapwood area basis' in the terminology of Edwards et al. (1996)), as $V_s = V \cdot \rho_b(c_w + m_c c_s)/(\rho_s c_s)$, where ρ_b is the basic density of wood (0.5 g cm^{-3} for the studied trees), c_w and c_s are specific heat capacities of the wood matrix (1200 J kg^{-1} K^{-1}) and sap water (4182 J kg^{-1} K^{-1}), respectively, m_c (g g^{-1}) is the water content of sapwood (1.1 for the trees) and ρ_s is the density of sap (10^{-3} kg cm^{-3}). Second, we scaled the resulting single-point estimates of sap flux to whole-tree sap flow (F, kg h^{-1}) empirically, by multiplying by estimated sapwood area (a, cm^2) and sap density ρ_s, and then using direct measurements of whole-tree sap flow by lysimetry to produce an empirical calibration coefficient (f, unitless). Thus, $F = fa\rho_s V_s$. As comparisons of sap flow methods to lysimetry are best made when flows of water into or out of water storage tissues are smallest, typically during the middle of the day (Chuang et al. 2006, Buckley et al. 2011, Deng et al. 2017), we chose f for each tree to make mid-day maximum values of F match between sap flow and lysimetry (Table S1 available as Supplementary data at *Tree Physiology* Online presents values of a and f for each tree).

The empirical coefficient f incorporates two sources of potential divergence between point measurements of V_s and whole-tree sap flow: spatial variation in V_s (radial and/or azimuthal) and effects of drilling wounds. The fact that a single proportionality constant was sufficient to encompass these factors (f was nearly constant for each tree from February through May 2016; Table S1 available as Supplementary data at *Tree Physiology* Online) has two implications. First, it suggests that any radial or azimuthal variation that may have occurred in sap flux did not change systematically over time, such that our point measurements remained proportional to the true spatial mean of V_s within each tree. Second, it suggests that any wounding effects that may have occurred did not generate nonlinearity in the relationship between V_s and F in our trees. Future efforts to apply the DRM more broadly, and without the benefit of lysimetric calibration, may benefit from numerical simulations of flow in a three-sensor system to determine whether wound correction models derived for two-sensor systems in previous studies (Swanson and Whitfield

1981, Burgess et al. 2001) are suitable for our three-sensor configuration.

Results

Theoretical testing

Operational procedures for DRM We calculated V_{DRM} by averaging values (measured at 1 Hz) for window sizes varying between 5 and 100 s, with the central time point chosen as that at which either σ_{12} or σ_{23} was smallest. Monte Carlo simulations indicated that the optimal window size was inversely related to sap velocity (Figure 3). For example, SEs were smallest using a window width of 80–100 s for a true sap velocity of 30 cm h^{-1}, but using a width of 20–40 s when velocities were 80 cm h^{-1} (Figure 3b and e). Time windows for the least biased estimates of V did not overlap as indicated by the SE at $V = 80$ cm h^{-1} when comparing time windows of 20 and 80 s (Figure 3e and f). This is due to the assumption of an instantaneous heat pulse in the Marshall Model, from which all heat-pulse-based methods are derived (see Discussion).

In theory, window sizes of 80 s can be used, but in practice, the quality of recorded temperature data deteriorates as temperatures level off and noise thus becomes increasingly prominent. For example, if we excluded temperature rises of less than 0.015 K (three times the standard deviation of temperature noise due to sensor resolution), sap velocities >80 cm h^{-1} could not be discerned using a 100-s window. Optimal window sizes generally decreased as flow rates increased. To simplify, we suggest using a fixed window of 40 s for V_{DRM} calculations—the same window size as recommended for the HRM.

The DRM algorithm identifies both the optimal size and timing of the averaging window. There is a distinct transition of optimal window size and timing in the range of velocities at which the intrinsic uncertainties of V_{12} and V_{23} are similar, which occurs at around ~20 cm h^{-1}. At lower sap velocities, V_{12} is less uncertain than V_{23} (hence $V_{DRM} = V_{12}$, Eq. (7)), giving an optimal averaging window 40 s wide and centered between 60 and 70 s (Figure 4)—very similar to the averaging window commonly used for the HRM (40 s wide and centered at 80 s, see Chen et al. (2012)). At intermediate sap velocities, V_{23} is less uncertain than V_{12} (hence $V_{DRM} = V_{23}$), and the optimal averaging window is centered at >200 s—roughly when the temperature traces for Probes #2 and #3 intersect (see blue and red lines in Figure 4). Note that the velocity at which V_{12} transitions to V_{23} will depend on conditions and will differ with probe positions and heat pulse strength and length. For example, greater heat intensity (Q/t_0) will lead to a transition at greater flux.

Performance of the heat-pulse-based methods Simulation results with synthetic data are shown in Figure 5. Among all four methods, the DRM calculation of V was consistently closest to the true value used to generate the synthetic data, deviating little from the true value for high (0.2% deviation at 80 cm h^{-1}), slow (0.5% at 20 cm h^{-1}) and negative sap velocities (1.6% at −10 cm h^{-1}). The coefficient of variation of estimates was also smallest for the DRM (e.g., 2% at 20 cm h^{-1} and 0.5% at 80 cm h^{-1}). The HRM performed well at negative to slow sap velocities (<40 cm h^{-1}) but systematically underestimated true sap velocity when velocity was high. The CHPM only performed well at intermediate sap velocities (20–40 cm h^{-1}), yielding a widely diverging range of estimates when true sap velocities were high, low or negative. The poor performance of the HRM and CHPM at high sap velocities was caused by very small temperature rises at the upstream temperature sensor (δ_1). Calculations that depend on δ_1 become unreliable under such conditions (Figure S3a available as Supplementary data at *Tree Physiology* Online). The CHPM also performs poorly when sap velocity is low because it relies on precise determination of the time when $\delta_1 = \delta_3$: δ_3 is small when sap velocity is low, leading to increased error (Figure S3b available as Supplementary data at *Tree Physiology* Online). The Tmax method is based on timing of peak temperature rise and is thus sensitive to noise at relatively slow sap velocities (e.g., 35% coefficient of variation at 20 cm h^{-1}).

CHPM and Tmax will perform better if noise reduction techniques are implemented, while HRM and DRM are less sensitive to noise. The applicable range of the HRM depends on magnitude of errors in measured temperatures (Figure S4 available as Supplementary data at *Tree Physiology* Online), which in turn depend on precision of the temperature sensor (σ_T) and the amount of heat generated during the heat pulse. The useful range of the HRM could be extended by increasing heat pulse duration or intensity.

Sensitivity to k Among the four heat-pulse methods, the HRM was the most sensitive to uncertainty in k. Calculations of V are directly proportional to k using the HRM Eq. (4). Estimates of V from the DRM are also sensitive to k at low sap velocities (<20 cm h^{-1}) because V_{DRM} is dominated by V_{12} (V_{HRM}, Eq. (4)) under such conditions (Figure 6). However, when sap velocity is high, V_{DRM} equals V_{23}, which is much less sensitive to k; this is because V_{23} is the sum of two terms, of which only one depends directly on k (Eq. (6)). Using k as estimated using either Eq. (13) or Eq. (14) considerably improves the accuracy of the DRM (and HRM) at low sap velocities. The CHPM is completely insensitive to uncertainty in k velocities.

Validating DRM with lysimetry

Peak transpiration fluxes were 5.5, 6.0 and 7.0 kg h^{-1}, for Trees #1, #2 and #3, respectively, from February to May

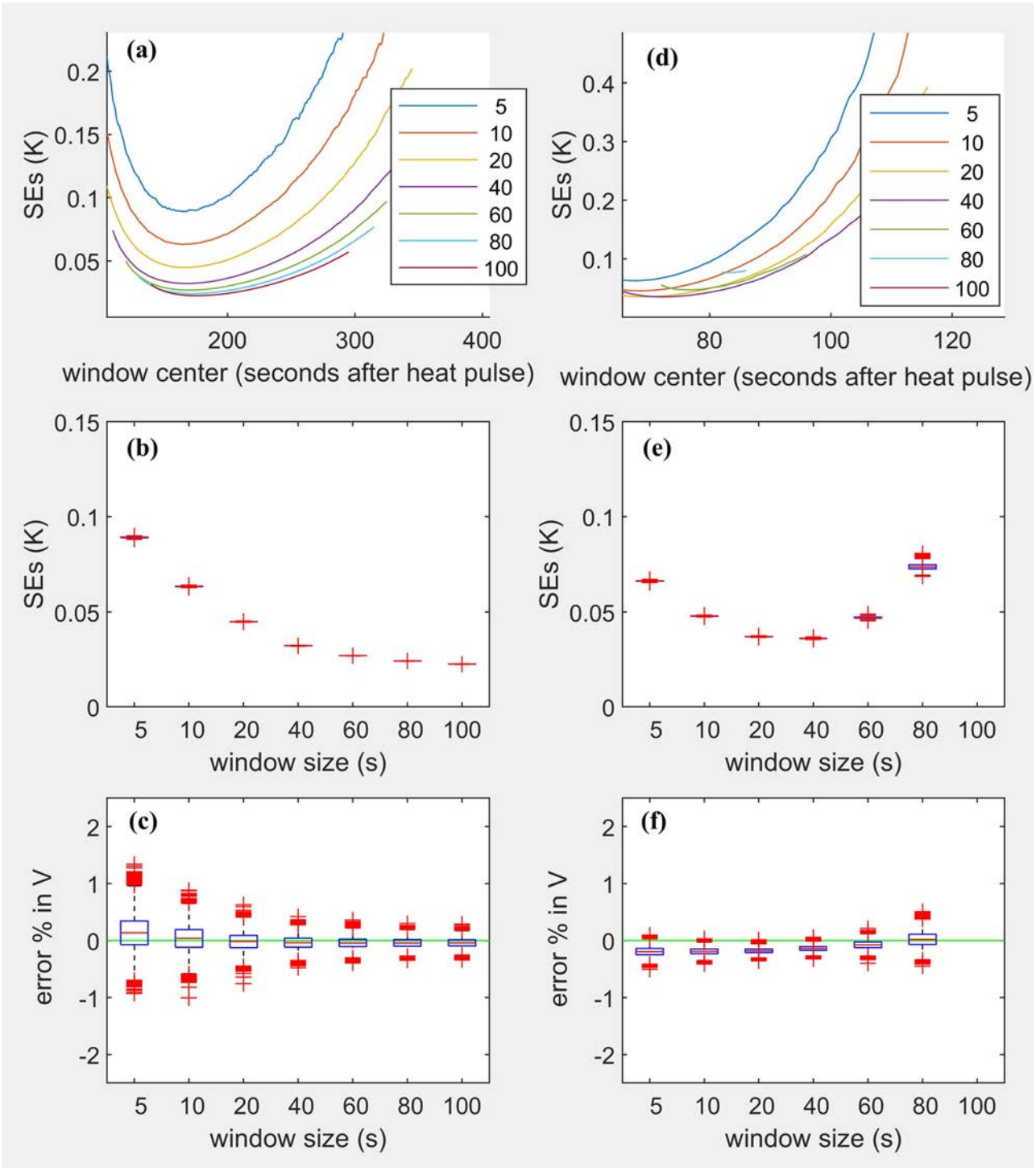

Figure 3. The SEs of averaging V_{DRM} over various sized windows are shown in (a) and (d) with their corresponding central time points on the *x* axis, (b) and (e) illustrate the distribution of SEs from 10,000 simulations in relation to the averaging window size, and the distribution of the estimation errors (%) in V_{DRM} to the width of the window are shown in (c) and (f). True sap velocity was set to 30 cm h^{-1} (a–c) or 80 cm h^{-1} (d–f). The legend values (5 to 100) for (a) and (d) specify width of the averaging window in seconds. The blue boxes (b, c, e, f) have upper and lower edges defined by the 25th and 75th percentiles of 10,000 runs and contain mean values denoted by the red lines. The red crosses are the outliers greater than 2.7 standard deviations from the mean.

2016. Peak temperature rise of Probe #2 was around 2 K at midday and 0.6 K at night. Peak sap velocity calculated by the DRM was >60 cm h^{-1} for Tree #1, >80 cm h^{-1} for Tree #2 and > 100 cm h^{-1} for Tree #3.

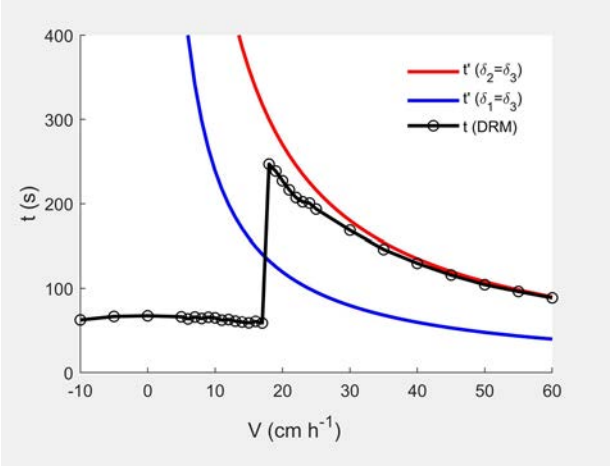

Figure 4. The time corresponding to the center of the optimal averaging window for the DRM varies with sap velocity. The thick red and blue solid lines are the theoretical times at which the temperature traces would intersect (red: $t' = (x_2 + x_3)/2V$ when $\delta_2 = \delta_3$ or $(x_1 + x_3)/2V$ when $\delta_1 = \delta_3$) in the absence of temperature noise. The solid black line and black symbols are theoretical values calculated with DRM in the absence of random noise.

The DRM reproduced diel patterns of sap flow measured by lysimetry under a wide range of flow conditions, from negligible flows at night to very large and fluctuating flows (see Figure 7 for sap flow, Figure 8 for heat pulse velocity of Tree #3 and Figure S5 available as Supplementary data at *Tree Physiology* Online for all three trees). The HRM, by contrast, was unable to capture heat pulse velocity >25 cm h^{-1} (>2 kg h^{-1}, Figure 7). While better than the HRM in capturing large sap velocities (Figures 7 and 8), the CHPM also failed when flows were very fast or very slow (see Figure 8). The Tmax method failed to capture heat pulse velocities <20 cm h^{-1}. To match peak velocity measured by lysimetry, scaling factors for Tmax had to be increased with time (see Table S1 available as Supplementary data at *Tree Physiology* Online). For example, scaling factors increased 1.3-fold from February to April, and 1.6-fold from February to May. The sensitivity of the Tmax method to noise and probe alignment requires constant adjustment of scaling factors as trees grow.

By comparison with lysimetry data, heat-based methods of measuring sap flow show a lag of ~10 min. A likely explanation is that water stored in stems and branches contributes to transpiration in the early morning—stores that are replenished via root water uptake in the late afternoon.

Discussion

The DRM vs other heat-pulse-based methods

The DRM presented here was more robust than other common heat pulse methods (HRM, CHPM and Tmax) across a wide range of sap velocities, in both theoretical and experimental tests. In theoretical tests, the DRM produced the least bias and smallest variance among the four methods. In experimental tests, the DRM accurately tracked diel trends in tree water use (as measured by lysimetry) from 0–7 kg h^{-1} or 0–100 cm h^{-1}.

The applicable upper limit for the HRM can be roughly estimated from Eq. (4), given the resolution of temperature sensors and peak rise in temperature. For example, if we assume:

- that the temperature rise at the upstream probe (δ_1) is reliable if its output is at least three times the standard deviation of temperature noise due to sensor resolution (approximately 0.005 K in our experiment), so that values of δ_1 below 0.015 K are excluded, and
- that the largest observed value of the temperature rises at the first downstream probe (δ_2) is 1.0 K,

then with a probe spacing of 1.5 cm and $k = 0.0025$ cm^2 s^{-1}, the upper limit of velocity that the HRM can estimate is

$$V_{HRM,max} = \frac{2 \cdot 0.0025 \text{ cm}^2\text{s}^{-1}}{1.5 \text{ cm}} \ln\left(\frac{1 \text{ K}}{0.015 \text{ K}}\right) = 0.014 \text{ cm s}^{-1} \ (\approx 50 \text{ cm h}^{-1}). \quad (15)$$

In practice, the minimum uncertainty in δ_1 is likely larger than the sensor resolution, due to other factors (e.g., background fluctuations, drifts in temperature). This limit could be increased by reducing probe spacing or increasing the size of the heat pulse. However, closer spacing magnifies relative errors caused by imperfect alignment of probes during installation.

The CHPM was unable to detect high sap velocities because, like the HRM, it is limited by uncertainty in δ_1. The CHPM also fails at low sap velocities because the intrinsic uncertainty in the 'crossover point' of δ_1 and δ_3 is greater. Both the CHPM and the Tmax method are inherently incapable of detecting negative sap velocities (reverse flows). Testi and Villalobos (2009) suggested the resolution of the CHPM could be improved using an empirical calibration function (Vandegehuchte and Steppe 2012*c*), although this requires study- and species-specific solutions. Pearsall et al. (2014) obtained estimates of sap velocity >200 cm h^{-1} by supplementing the HRM with the CHPM. Those velocities far exceed values that we were able to detect using the CHPM (~40–50 cm h^{-1}). A possible reason for this difference is that the values reported in their study were corrected for wounding, whereas ours were not. Given that Pearsall et al. (2014) used temperature sensors and dataloggers with similar resolution to ours, and heater probes with similar resistances (~18 Ω), this discrepancy in maximum velocities could also be due to wider probe spacing used in the present study (1.5 cm vs 1.2 cm used by Pearsall et al. 2014). To assess this possibility, we can use Eq. (1) to quantify the effect of probe spacing on the maximum temperature rise that one would expect to occur at the upstream probe (Probe #1). Suppose $\rho = 1.08 \cdot 10^3$ kg m^{-3}, $c = 2.8 \cdot 10^3$ J kg^{-1} K^{-1},

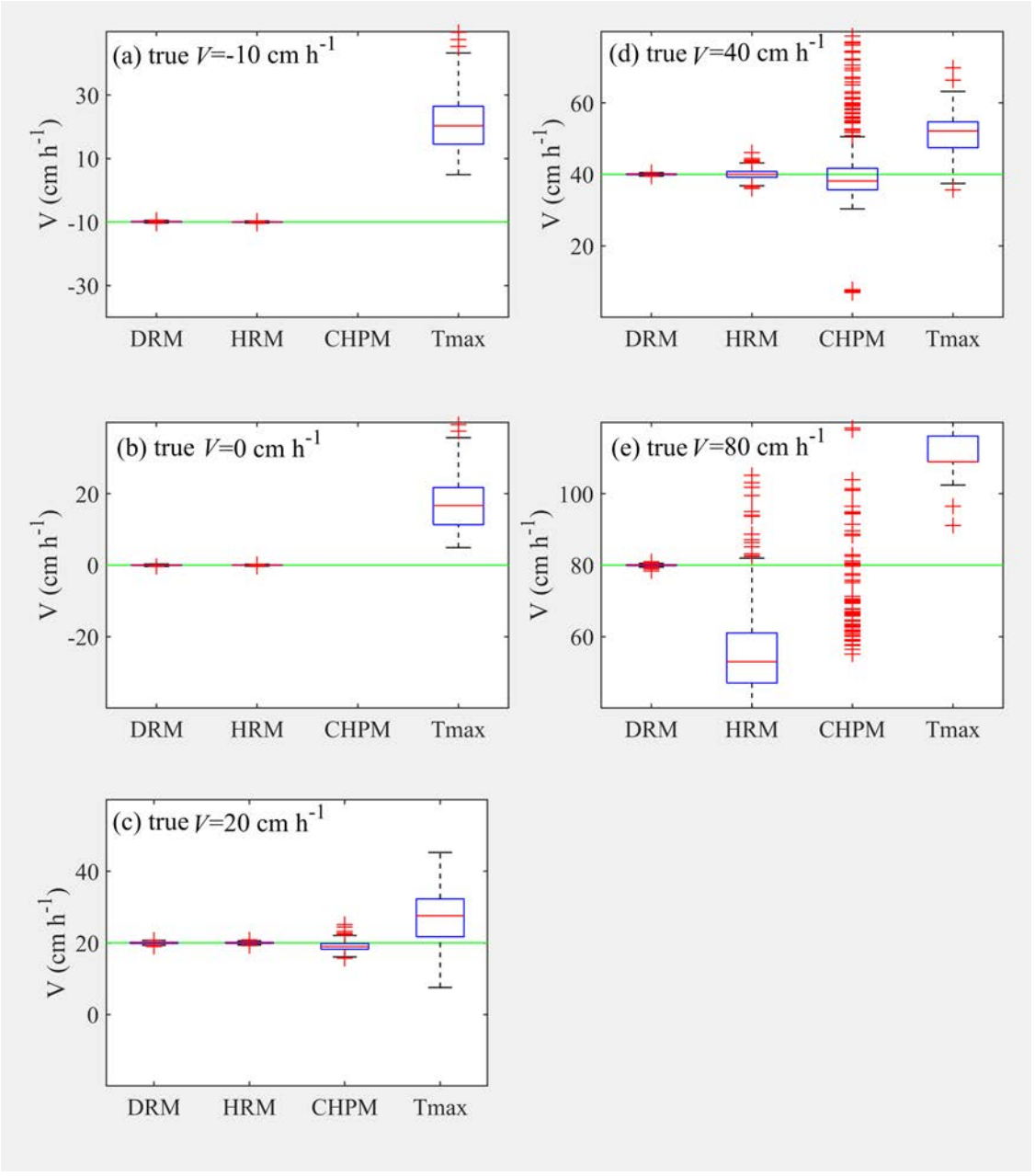

Figure 5. Boxplots showing the distributions of sap velocities (V, cm h^{-1}) calculated with the DRM, HRM, CHPM and Tmax methods from synthetic temperatures with Monte Carlo sampling of $\sigma_T = 0.02$ K, $t_0 = 10$ s and $m_c = 1.25$ g g^{-1}. The mean values are shown by red lines in the blue boxes, which have upper and lower edges defined by the 25th and 75th percentiles, and the red crosses are the outliers that are more than 2.7σ from the mean. The CHPM was not given in panels (a) and (b) as it could not resolve negative or low flows.

$Q = 1{,}370$ J m^{-1} (a 3.5-cm probe with 18 Ω resistance and 6 s pulse at 12 V), and $k = 0.0025$ cm^2 s^{-1}; then, at a true heat pulse velocity of 100 cm h^{-1} (0.028 cm s^{-1}), δ_1 should reach 0.0099 K for a probe spacing of 1.2 cm, and 0.0014 K for a spacing of 1.5 cm. This seven-fold difference results from the exponential dependence of temperature rise on probe spacing Eq. (1). We suggest that the superior performance of the DRM compared with the CHPM at high velocities in the current study was likely due to wider probe spacing in the current study. Wider spacing has the advantage that a given absolute error of probe alignment during installation will cause a smaller error in calculated sap velocity.

The DRM has other advantages. Most importantly, the measurement principle Eq. (2) is the same across all sap velocities. Switching measurement principles, as required if HRM is used for low velocities and the CHPM for high velocities, creates logistical problems. Secondly, the DRM provides a theoretical basis for identifying the optimal time window in which to average

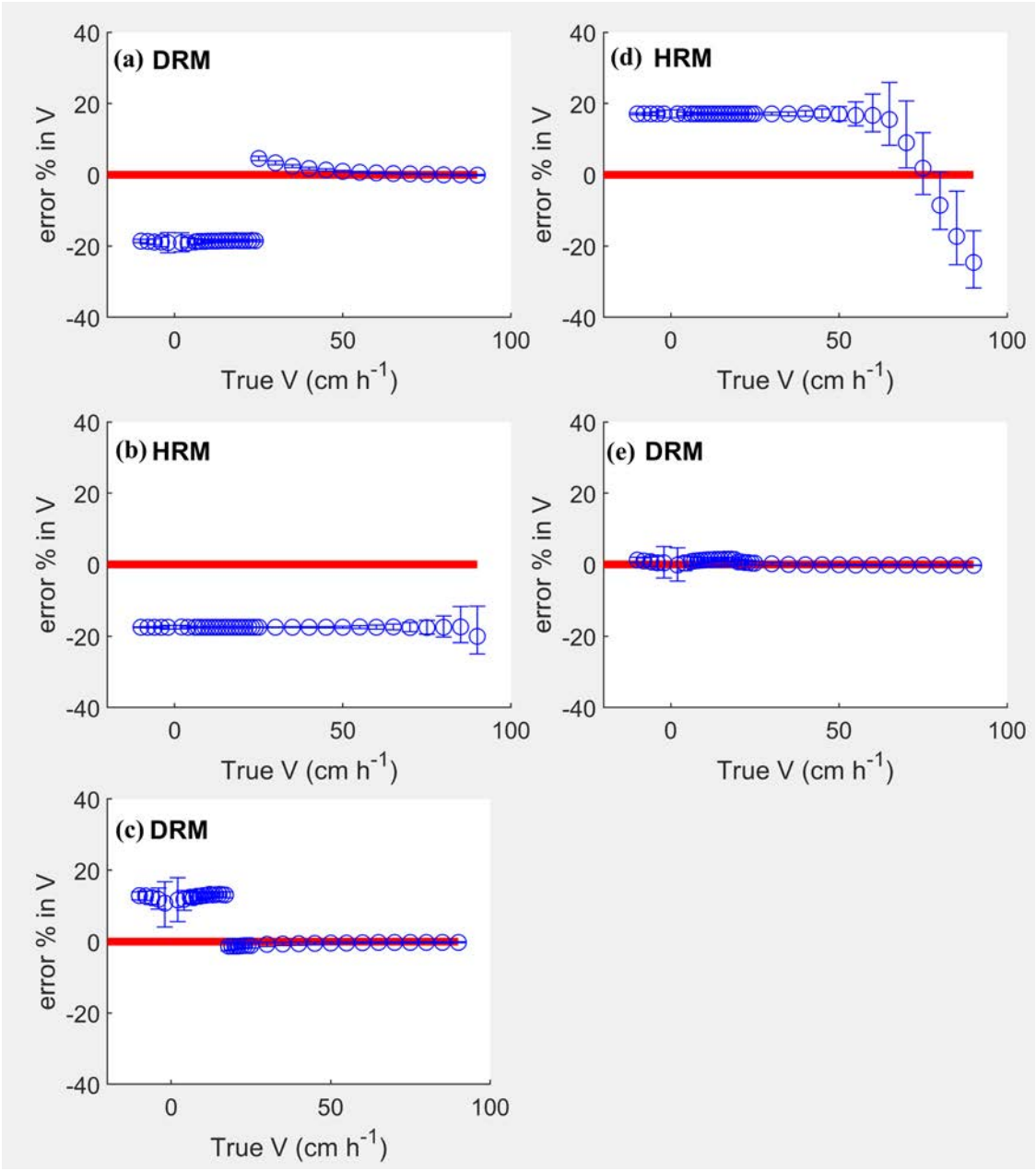

Figure 6. Uncertainties in V estimation due to k errors: true $k = 0.0024$ cm^2 s^{-1} (a–d), underestimation of V with the DRM (a) and HRM (b) using constant $k = 0.0021$ cm^2 s^{-1}, and overestimation with the DRM (c) and HRM (d) for constant $k = 0.003$ cm^2 s^{-1}. Errors in the corrected velocity using k estimated with the DRM are in (e). Note the underestimation at higher velocity with the HRM in (d) is a result of negative bias (see Figure 1).

estimates of sap velocity. We found an optimal window for *E. cypellocarpa* of 50–120 s after the heat pulse (Figure S6 available as Supplementary data at *Tree Physiology* Online, which is approximately equal to theoretically calculated values (Figure 4) and similar to the window used for the HRM (60–100 s). Thirdly, the DRM is less sensitive to noise than the CHPM, because the latter relies on a single intersection point, whereas the former averages data over a longer time period. Finally, unlike the HRM, the DRM is relatively insensitive to uncertainty in the value of k when $V > 20$ cm h^{-1} because $V_{DRM} = V_{23}$ Eq. (6) at high sap velocities, and the term involving k in Eq. (6) becomes small compared to the term that involves t.

Impact of the finite heat pulse length

Following Marshall's original model, the assumption of an instantaneous heat pulse results in biased estimates of sap velocity in most methods. A small negative bias is evident in both the DRM- and HRM-based velocity estimates. The bias of the DRM increases from −0.03% when $V = 30$ cm h^{-1} to −0.2% when

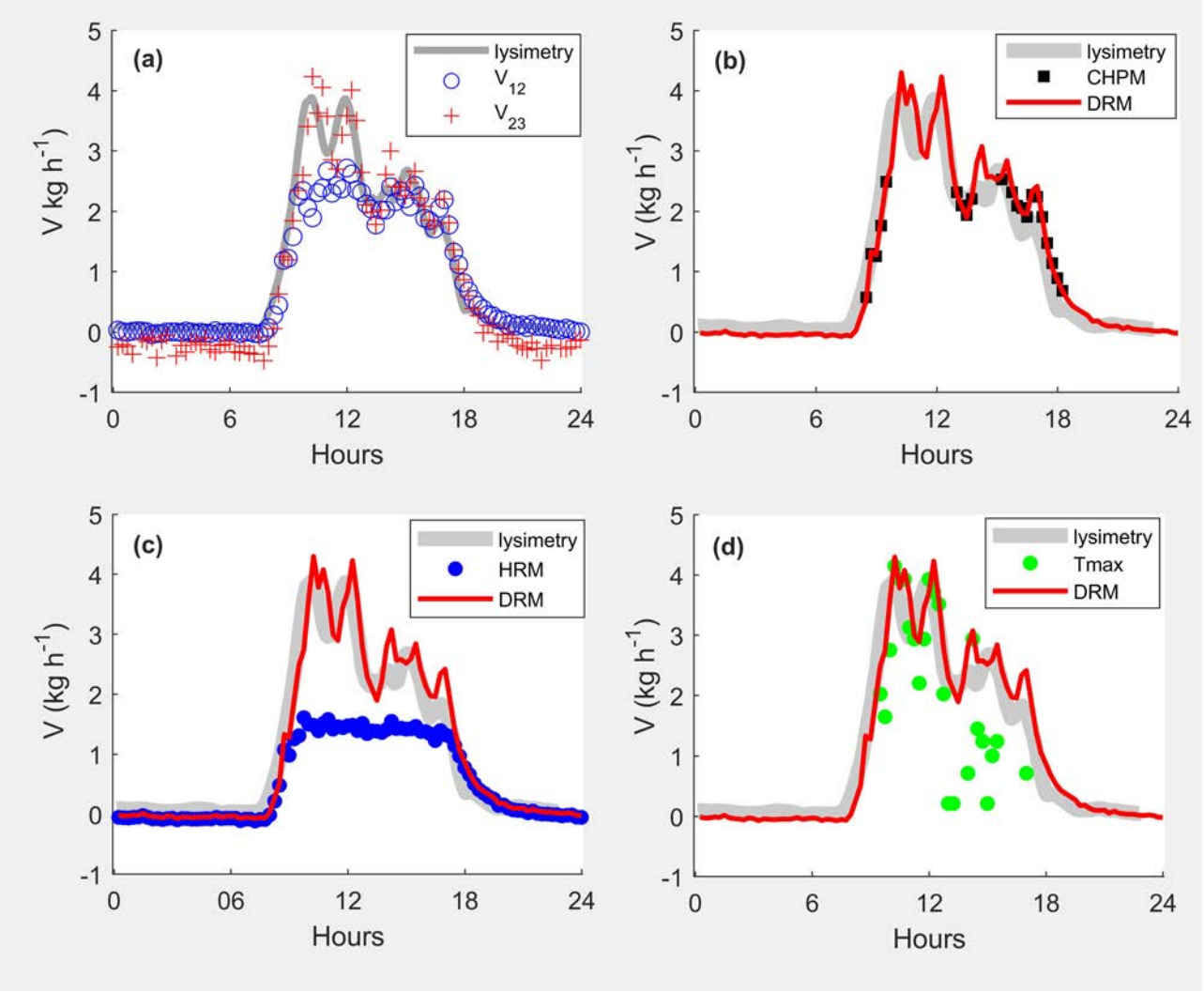

Figure 7. Comparison of lysimeter data (gray lines) with sap flow calculated using the DRM (red line) CHPM (black symbols), HRM (blue symbols) and Tmax (green symbols), for Tree #3 on 18 April 2016.

$V = 80$ cm h^{-1} (Figure 9). A larger bias is evident using the CHPM (which underestimates velocity by 9% at 30 cm h^{-1}) because of its reliance on the precise time at which $\delta_1 = \delta_3$. Its high sensitivity to pulse duration (t_0) was also recognized in a data synthesis study by Flo et al. (2019), though the Tmax method can be modified to account for t_0 (Kluitenberg and Ham 2004), thus eliminating this bias. In practice, Tmax-based sap velocity estimates are highly uncertain when velocity is high, due to sensitivity to noise (Figure 5e). Shifting t_0 helps mitigate the impact of the finite heat pulse length across methods, resulting in negligible bias for the DRM (Figure 9).

Misalignment correction

Misalignment of probes is a major source of uncertainty for heat-pulse techniques. It affects all methods and can bias inferred sap velocity either positively or negatively. Burgess et al. (2001) noted two alternative scenarios that could be used in misalignment corrections in the HRM: either that Probe 1 is misaligned, or that Probe 2 is misaligned. Corrections are calculated for each case and are used to force calculated sap velocity to equal zero under conditions when the true sap velocity is known to be zero. Burgess et al. (2001) recommended using the average of the two corrections. However, though all three methods result in matched calculated and measured sap velocities under 'zero-flow' conditions, they do not yield consistent day-time sap velocities (Figure 10).

The HRM requires a known value of k to correct errors due to probe misalignment. Typically, a constant k is assumed. Burgess et al. (2001) used the Tmax method Eq. (15) to calculate k. This is a somewhat circular procedure because the Tmax method requires knowledge of probe locations. It would be preferable to concurrently solve for all three unknowns–Δx_1, Δx_2 and k—as shown by Chen et al. (2012). Such a

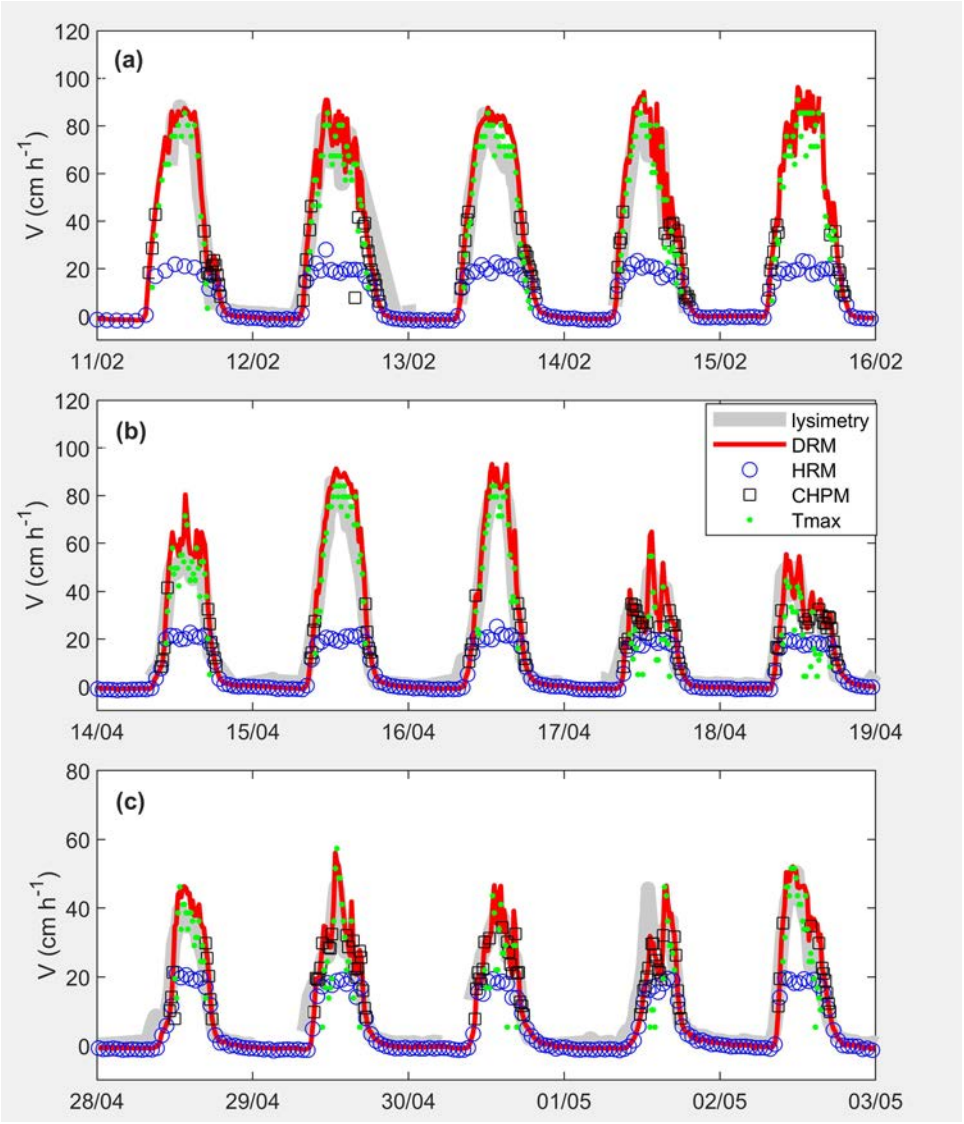

Figure 8. The heat pulse velocity calculated with DRM and other heat-pulse-based methods over the months for Tree 3; results for other trees are shown in Figure S5. available as Supplementary data at *Tree Physiology* Online X-axis is date in the format of dd/mm in 2016.

calibration approach may not be achievable unless constrained with assumptions or additional calculations (e.g., sap velocity independently inferred via an empirical function in Chen et al. (2012)). We developed an alternative calibration procedure (Methods S4 available as Supplementary data at *Tree Physiology* Online), in which alignment is first checked using the HRM method suggested by Burgess et al. (2001), the non-unique solution is then constrained by comparing velocities using the CHPM, which is independent of k, and finally k is identified using the Tmax method under zero-flow conditions. When the average solution is chosen from the HRM method, sap velocities estimated using the DRM match well with those estimated using the CHPM (Figure 11). In this scenario, any misalignment is well corrected (CHPM is sensitive to misalignment) and k is appropriately estimated (DRM is sensitive to k at low flow).

The three-probe approach used by the DRM allows diagnosis of misalignment corrections. Combined with calculations based on the CHPM, it also allows for determination of both k and misalignment under moderate conditions (e.g., typical day time).

Conclusions

We present a new heat-pulse-based method, the DRM, to calculate sap velocity in woody plants. We demonstrate both theoretically and experimentally that the DRM can effectively measure a broader range of sap velocities than other common heat-pulse-based methods. Like an earlier approach that combined the HRM and CHPM (Pearsall et al. 2014), the DRM computes two distinct estimates of sap velocity at each time point; however, the DRM has several advantages, including a theoretical basis for selecting between the two velocity estimates and for identifying

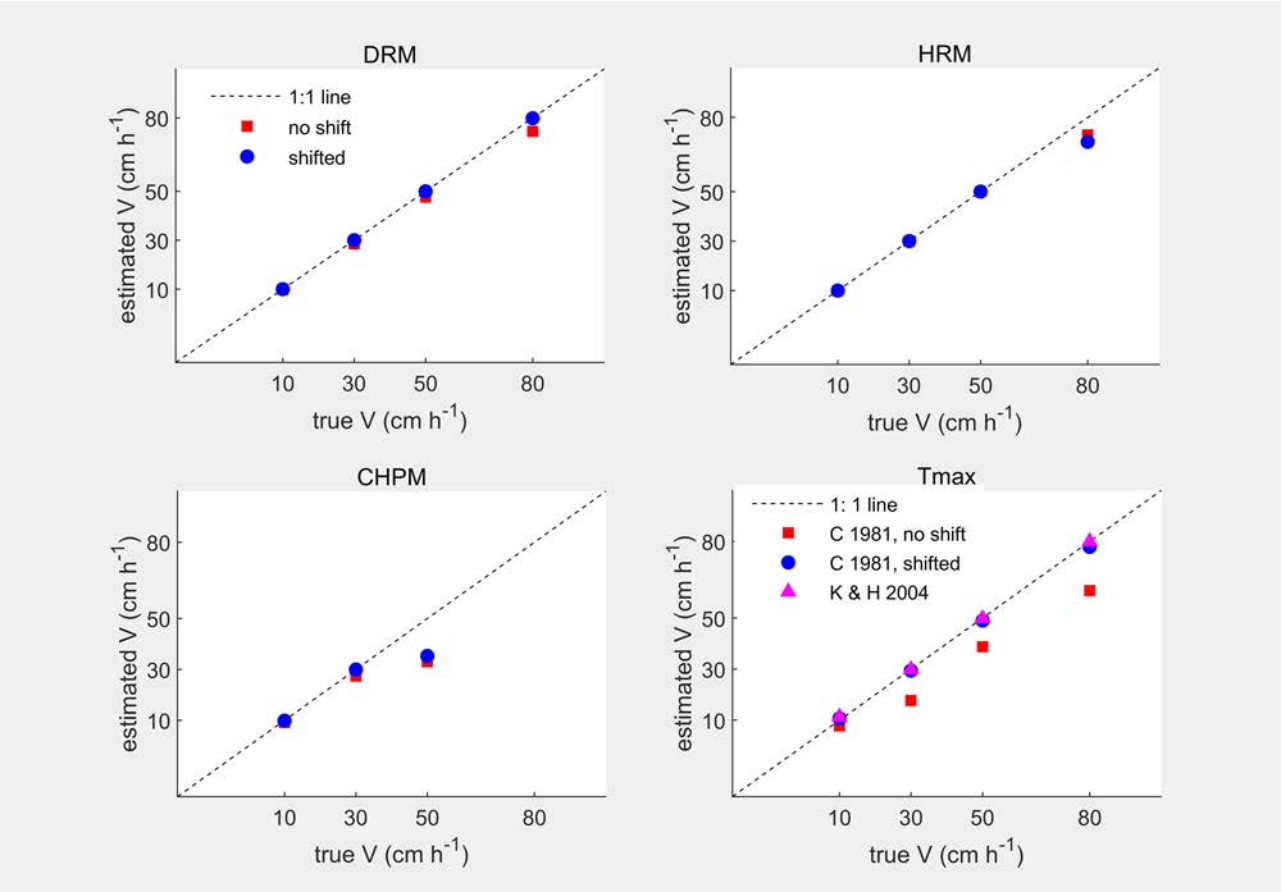

Figure 9. Comparison between heat-pulse-based methods without the time shift (red squares) and with the shift (blue circles) to account for finite heat pulse duration (t_0). The original Tmax (Cohen et al. 1981) and the CHPM (Green and Clothier 1988) were shown without the t_0 shift in red and with the shift in blue. The modified Tmax method of Kluitenberg and Ham (2004) is shown in magenta triangles. Each calculation is averaged from 10,000 Monte Carlo simulations (at $\sigma_T = 0.02$ K, $t_0 = 15$ s, $q = Q/t_0 = 80$ J m^{-1} s^{-1}, $k = 0.002$ cm^2 s^{-1}, $m_c = 1.25$ g g^{-1}, $\rho_b = 0.5{\cdot}10^3$ kg m^{-3}).

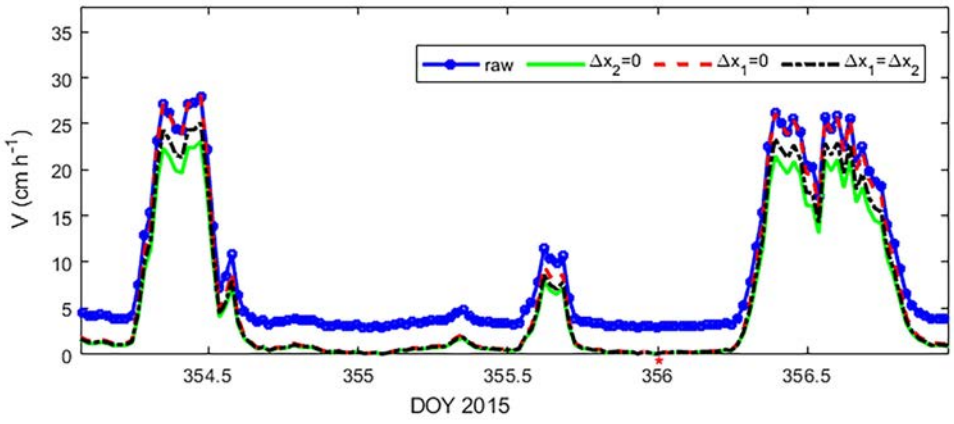

Figure 10. Divergence in corrected velocities after misalignment corrections in the HRM method following Burgess et al. (2001). The blue points show the raw data without misalignment correction. $\Delta x_1 = 0$ assumes no misalignment of x_1 and only x_2 is corrected. Similarly, $\Delta x_2 = 0$ means that only x_1 is corrected and $\Delta x_1 = \Delta x_2$ is the average of the solutions when either x_2 or x_1 is corrected. Corrections were applied to make the calculated flow rate equal to zero at the time indicated with a red asterisk; we reasoned that the true flow rate was zero at that time because a large rain event had occurred in the 12 h prior, and reported flow had been steady for several hours.

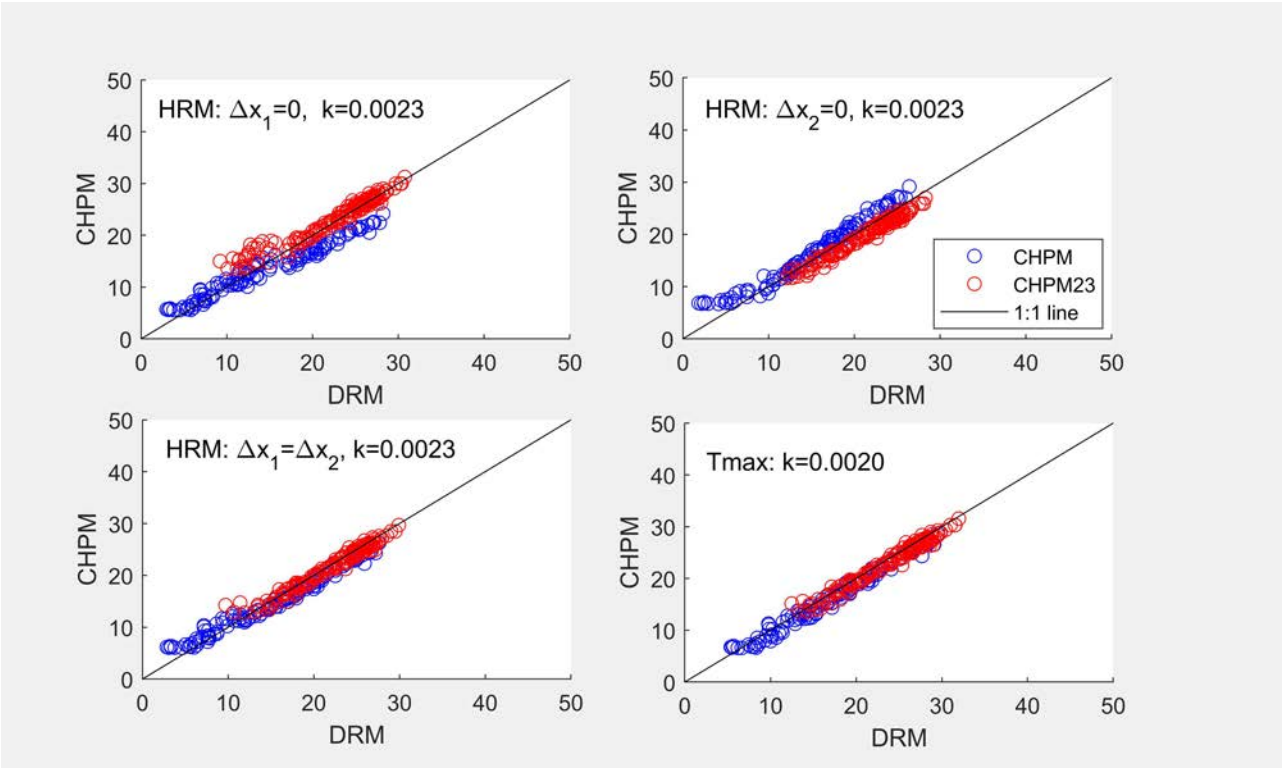

Figure 11. Examples of the misalignment correction procedure with the HRM and Tmax method at both zero-flow conditions and constrained by the CHPM (Eq. (11)) at modest flow rate condition (sap velocities given in cm h^{-1}). Annotations 'HRM: $\Delta x_1 = 0$, $k = 0.0023$' mean that the misalignment is calibrated solely on x_2 at $k = 0.0023$ cm^2 s^{-1} with the HRM method. CHPM23 refers to Eq. (6) where $\delta_2 = \delta_3$. See details of the misalignment correction procedure in Methods S4 available as Supplementary data at *Tree Physiology* Online.

the optimal times for averaging data, and a reduced sensitivity to noise at high velocities.

Supplementary data

Supplementary data for this article are available at *Tree Physiology* Online.

Conflict of interest

The authors have no conflict of interest.

Funding

This work was supported by the Australian Research Council (LP130100183), the International Wheat Yield Partnership (IWYP, project 89) through a grant from the Grains Research and Development Corporation (GRDC, US00082), the National Science Foundation (Awards #1557906 and 1951244), the Almond Board of California and the USDA National Institute of Food and Agriculture (Hatch project 1016439 and Grant #2020-67013-30913).

Authors' contributions

T.N.B., M.A.A. and Z.D. planned, designed and coordinated the research. T.N.B. developed the DRM algorithm and designed and built the probes for the experiment. Z.D. conducted the numerical simulations, lysimetry experiment, data collection, analysis and interpretation, with assistance and feedback from T.N.B. H.K.V. and M.E.G. performed part of the experiment and data collection. Z.D. and T.N.B. wrote the manuscript. All authors edited successive drafts of the manuscript.

References

Bleby T, McElrone A , Burgess S (2008) Limitations of the HRM: great at low flow rates, but not yet up to speed. In: 7th International Workshop on Sap Flow: Book of Abstracts. International Society of Horticultural Sciences, Seville, Spain.

Buckley TN, Turnbull TL, Pfautsch S, Adams MA (2011) Nocturnal water loss in mature subalpine *Eucalyptus delegatensis* tall open forests and adjacent *E. pauciflora* woodlands. Ecol Evol 1:435–450.

Buckley TN, Turnbull TL, Pfautsch S, Gharun M, Adams MA (2012) Differences in water use between mature and post-fire regrowth stands of subalpine *Eucalyptus delegatensis* R. Baker. For Ecol Manage 270:1–10.

Burgess SS, Adams MA, Turner NC, Beverly CR, Ong CK, Khan AA, Bleby TM (2001) An improved heat pulse method to measure low and reverse rates of sap flow in woody plants. Tree Physiol 21:589–598.

Cermak J, Kucera J, Bauerle WL, Phillips N, Hinckley TM (2007) Tree water storage and its diurnal dynamics related to sap flow and changes in stem volume in old-growth Douglas-fir trees. Tree Physiol 27:181–198.

Chen X, Miller GR, Rubin Y, Baldocchi DD (2012) A statistical method for estimating wood thermal diffusivity and probe geometry using in situ heat response curves from sap flow measurements. Tree Physiol 32:1458–1470.

Chuang YL, Oren R, Bertozzi AL, Phillips N, Katul GG (2006) The porous media model for the hydraulic system of a conifer tree: linking sap flux data to transpiration rate. Ecol Model 191:447–468.

Clearwater M, Meinzer F, Andrade J, Goldstein G, Holbrook N (1999) Potential errors in measurement of nonuniform sap flow using heat dissipation probes. Tree Physiol 19:681–687.

Cohen Y, Fuchs M, Green G (1981) Improvement of the heat pulse method for determining sap flow in trees. Plant Cell Environ 4:391–397.

Deng Z, Guan H, Hutson J, Forster MA, Wang Y, Simmons CT (2017) A vegetation-focused soil-plant-atmospheric-continuum model to study hydrodynamic soil-plant water relations. Water Resour Res 53:4965–4983.

Edwards WRN, Becker P, Èermák J (1996) A unified nomenclature for sap flow measurements. Tree Physiol 17:3.

Flo V, Martinez-Vilalta J, Steppe K, Schuldt B, Poyatos R (2019) A synthesis of bias and uncertainty in sap flow methods. Agric For Meteorol 271:362–374.

Forster MA (2019) The dual method approach (DMA) resolves measurement range limitations of heat pulse velocity sap flow sensors. Forests 10:46.

Forster MA (2020) The importance of conduction versus convection in heat pulse sap flow methods. Tree Physiol 40:683–694.

Granier A (1985) Une nouvelle méthode pour la mesure du flux de sève brute dans le tronc des arbres. In: Annales des Sciences forestières. EDP Sciences Les Ulis, France, pp 193–200.

Green S, Clothier B (1988) Water use of kiwifruit vines and apple trees by the heat-pulse technique. J Exp Bot 39:115–123.

Green S, Clothier B, Jardine B (2003) Theory and practical application of heat pulse to measure sap flow. Agron J 95:1371–1379.

Kluitenberg GJ, Ham JM (2004) Improved theory for calculating sap flow with the heat pulse method. Agric For Meteorol 126:169–173.

López-Bernal Á, Alcántara E, Villalobos FJ (2014) Thermal properties of sapwood of fruit trees as affected by anatomy and water potential: errors in sap flux density measurements based on heat pulse methods. Trees 28:1623–1634.

Lopez-Bernal A, Testi L, Villalobos F (2017) A single-probe heat pulse method for estimating sap velocity in trees. New Phytol 216:321–329.

Marshall D (1958) Measurement of sap flow in conifers by heat transport. Plant Physiol 33:385.

Nadezhdina N, Cermak J, Nadezhdin V (1998) Heat field deformation method for sap flow measurements. In: Measuring sap flow in intact plants. Proceedings of 4th International Workshop. Mendel University, Brno, Czech Republic, pp 72–92.

Pearsall KR, Williams LE, Castorani S, Bleby TM, McElrone AJ (2014) Evaluating the potential of a novel dual heat-pulse sensor to measure volumetric water use in grapevines under a range of flow conditions. Funct Plant Biol 41:874–883.

Pfautsch S, Keitel C, Turnbull TL, Braimbridge MJ, Wright TE, Simpson RR, O'Brien JA, Adams MA (2011) Diurnal patterns of water use in *Eucalyptus victrix* indicate pronounced desiccation-rehydration cycles despite unlimited water supply. Tree Physiol 31:1041–1051.

Ren R, von der Crone J, Horton R, Liu G, Steppe K (2020) An improved single probe method for sap flow measurements using finite heating duration. Agric For Meteorol 280:107788.

Steppe K, Vandegehuchte M, Tognetti R, Mencuccini M (2015) Sap flow as a key trait in the understanding of plant hydraulic functioning. Tree Physiol 35:341–345.

Swanson RH, Whitfield DWA (1981) A numerical analysis of heat pulse velocity theory and practice. J Exp Bot 32:221–239.

Testi L, Villalobos FJ (2009) New approach for measuring low sap velocities in trees. Agric For Meteorol 149:730–734.

Vandegehuchte MW, Steppe K (2012*a*) A triple-probe heat-pulse method for measurement of thermal diffusivity in trees. Agric For Meteorol 160:90–99.

Vandegehuchte MW, Steppe K (2012*b*) Improving sap flux density measurements by correctly determining thermal diffusivity, differentiating between bound and unbound water. Tree Physiol 32:930–942.

Vandegehuchte MW, Steppe K (2012*c*) Sapflow+: a four-needle heat-pulse sap flow sensor enabling nonempirical sap flux density and water content measurements. New Phytol 196:306–317.

Wilson KB, Hanson PJ, Mulholland PJ, Baldocchi DD, Wullschleger SD (2001) A comparison of methods for determining forest evapotranspiration and its components: sap-flow, soil water budget, eddy covariance and catchment water balance. Agric For Meteorol 106:153–168.